REPORT SD TR 89 59

(4)

Chemical Interaction of Mn With the MoS_2 (0001) Surface Studied by High-Resolution Photoelectron Spectroscopy

J. R. LINCE, T. B. STEWART, and P. D. FLEISCHAUER
Chemistry and Physics Laboratory
The Aerospace Corporation
El Segundo, CA 90245

J. A. YARMOFF
Surface Science Division
National Institute of Standards and Technology
Gaithersburg, MD 20899

A. TALEB-IBRAHIMI
IBM T. J. Watson Research Center
Yorktown Heights, NY 10598

8 August 1989

Prepared for

SPACE SYSTEMS DIVISION
AIR FORCE SYSTEMS COMMAND
Los Angeles Air Force Base
P.O. Box 92960
Los Angeles, CA 90009-2960

This report was submitted by The Aerospace Corporation, El Segundo, CA 90245, under Contract No. F04701-88-C-0089 with the Space Systems Division, P. O. Box 92960, Los Angeles, CA 90009. It was reviewed and approved for The Aerospace Corporation by S. Feuerstein, Director, Chemistry and Physics Laboratory. Lt Carl Maes was the Air Force project officer for the Mission-Oriented Investigation and Experimentation (MOIE) program.

This report has been reviewed by the Public Affairs Office (PAS) and is releaseable to the National Technical Information Service (NTIS). At NTIS, it will be available to the general public, including foreign nationals.

This technical report has been reviewed and is approved for publication. Publication of this report does not constitute Air Force approval of the report's findings or conclusions. It is published only for the exchange and stimulation of ideas.

Carl J. Maes

CARL MAES, LT, USAF
MOIE Project Officer
SSD/CWDE

James A. Beres

JAMES A. BERES, LT COL, USAF
MOIE Program Manager
AFSTC/WCO OL-AB

UNCLASSIFIED

SECURITY CLASSIFICATION OF THIS PAGE

REPORT DOCUMENTATION PAGE

1a. REPORT SECURITY CLASSIFICATION Unclassified	1b. RESTRICTIVE MARKINGS
2a. SECURITY CLASSIFICATION AUTHORITY	3. DISTRIBUTION/AVAILABILITY OF REPORT Approved for public release; distribution unlimited.
2b. DECLASSIFICATION/DOWNGRADING SCHEDULE	
4. PERFORMING ORGANIZATION REPORT NUMBER(S) TR-0089(4945-03)-1	5. MONITORING ORGANIZATION REPORT NUMBER(S) SD-TR-89-59
6a. NAME OF PERFORMING ORGANIZATION The Aerospace Corporation Laboratory Operations 6b. OFFICE SYMBOL (If applicable)	7a. NAME OF MONITORING ORGANIZATION Space Systems Division
6c. ADDRESS (City, State, and ZIP Code) El Segundo, CA 90245-4691	7b. ADDRESS (City, State, and ZIP Code) Los Angeles Air Force Base Los Angeles, CA 90009-2960
8a. NAME OF FUNDING/SPONSORING ORGANIZATION 8b. OFFICE SYMBOL (If applicable)	9. PROCUREMENT INSTRUMENT IDENTIFICATION NUMBER F04701-88-C-0089
8c. ADDRESS (City, State, and ZIP Code)	10. SOURCE OF FUNDING NUMBERS PROGRAM ELEMENT NO. / PROJECT NO. / TASK NO. / WORK UNIT ACCESSION NO.

11. TITLE (Include Security Classification)
The Chemical Interaction of Mn With the MoS_2(0001) Surface Studied by High-Resolution Photoelectron Spectroscopy

12. PERSONAL AUTHOR(S)
Lince, Jeffery R., Stewart, Thomas B., Fleischauer, Paul D. (The Aerospace Corp.);

13a. TYPE OF REPORT	13b. TIME COVERED FROM _____ TO _____	14. DATE OF REPORT (Year, Month, Day)	15. PAGE COUNT
		1989 August 8	26

16. SUPPLEMENTARY NOTATION

17. COSATI CODES		
FIELD	GROUP	SUB-GROUP

18. SUBJECT TERMS (Continue on reverse if necessary and identify by block number)
Molybdenum Disulfide
X-ray Photoelectron Spectroscopy
Solid Lubrication
(continued)

19. ABSTRACT (Continue on reverse if necessary and identify by block number)

The interface produced by vapor deposition of Mn on the MoS_2(0001) surface was studied in situ by high-resolution photoelectron spectroscopy (PES) using synchrotron radiation. The evolution of the Mo-3d, Mn-3p, and S-2p core levels and of the valence band spectra during growth of thin films (10-58 Å) is consistent with partial conversion of the Mn overlayer to MnS by the overall reaction $2Mn + MoS_2 \rightarrow 2MnS + Mo$. The persistence of the substrate components of the Mo-3d and S-2p spectra for thicknesses >35 Å are consistent with the Volmer-Weber growth mode. Annealing a 58 Å film to 770 K resulted in an overlayer film consisting mostly of MnS coexisting with some metallic Mn. Analysis of the Mo-3d core levels indicates the production of a MoS_2(0001) surface with vacancy defects. Annealing to temperatures between 850 and 1040 K drove the reaction to completion (as shown by the valence band and Mn-3p core level spectra). Annealing of the sample to 1130 K resulted in uncovering the MoS_2(0001) surface due to breakup of the reacted layer. In addition, low energy electron diffraction (LEED) indicated the formation of (0001)-2×2 regions on the surface. This surface structure is interpreted in terms of an ordered MoS_{2-x} sulfur vacancy defect structure rather than a Mn-Mo-S compound.

Keywords: Solid Lubrication

20. DISTRIBUTION/AVAILABILITY OF ABSTRACT	21. ABSTRACT SECURITY CLASSIFICATION
☒ UNCLASSIFIED/UNLIMITED ☐ SAME AS RPT. ☐ DTIC USERS	Unclassified
22a. NAME OF RESPONSIBLE INDIVIDUAL	22b. TELEPHONE (Include Area Code) / 22c. OFFICE SYMBOL

DD FORM 1473, 84 MAR

83 APR edition may be used until exhausted.
All other editions are obsolete

SECURITY CLASSIFICATION OF THIS PAGE
UNCLASSIFIED

12. PERSONAL AUTHOR(S) (Continued)

Yarmoff, Jory A. (National Institute of Standards and Technology); and Taleb-Ibrahimi, Amina (IBM T. J. Watson Research Center).

18. SUBJECT TERMS (Continued)

Adhesion
Manganese
Interfacial Chemistry
Metal/Semiconductor Interfaces

PREFACE

This work was supported predominantly by Air Force Systems Command, Space Systems Division, Contract Number F04701-85-C-0086. Research was carried out in part at the National Synchrotron Light Source, Brookhaven National Laboratory, which is supported by the U. S. Department of Energy, Division of Materials Sciences and Division of Chemical Sciences (DOE contract number DE-AC02-76CH00016).

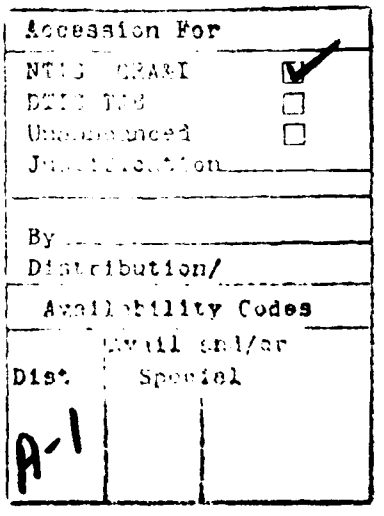

CONTENTS

TABLES

FIGURES

I. INTRODUCTION

The interaction of transition metals with MoS_2 surfaces has been increasingly studied recently with respect to applications in catalysis,[1] electronics materials,[2,3] and tribology (lubrication).[4] Especially well studied is the chemistry at the metal/MoS_2(0001) interface. This surface of MoS_2 is remarkable because of the highly anisotropic MoS_2 crystal structure. MoS_2 crystallizes in layers of S-Mo-S "sandwiches," within which the bonds are covalent, but each layer is bonded to the next one by relatively weak van der Waals' forces. As a result, its basal plane [or (0001)] surface, produced by cleaving between these layers, is relatively inert with respect to metal deposition.

The expected reaction of metals with MoS_2 to form metal sulfides is as follows:

$$Me + \frac{b}{2a} MoS_2 \rightarrow \frac{1}{a} Me_aS_b + \frac{b}{2a} Mo \qquad (1)$$

The free energy of reaction per metal atom (or ΔG_{rxn}) indicates that, at room temperature, a large number of metals are able to form sulfides based on bulk, equilibrium thermodynamics.[2,3] However, the work of McGovern, et al.,[3] Lince, et al.,[2,4] and Kamaratos, et al.,[1,5,6] indicates that, although a negative or small positive ΔG_{rxn} is a necessary condition for chemical reaction in this system, it is not sufficient as an indicator of reactivity at room temperature. Of the metals studied that correspond to this thermodynamic condition (i.e., are expected to chemically react with MoS_2), Al,[2,3] Cu,[3] In,[2,3] Pd,[2,5] and V[2] do not react, Fe[1,4] and Ni[3] exhibit minimal reactivity (Ni might be nonreactive),[6] and only Mg,[2,3] Ti,[2,3] and Mn[2] exhibit strong reactivity, i.e., decomposition of the substrate into metallic molybdenum and metal sulfide. Therefore, there are kinetic constraints in this system due to the structure of the individual metals in addition to the anisotropic structure of the MoS_2(0001) surface.

To investigate the chemistry of the more reactive interfaces in greater detail, we conducted a study of the interaction of thin films of Mn with the $MoS_2(0001)$ surface. The techniques we used are (a) core level and valence band photoelectron spectroscopies excited by synchrontron radiation, and (b) low energy electron diffraction (LEED). The use of synchrotron radiation allows for control of the electron escape depth by varying the photon energy. In addition, the use of a small line-width monochromator and a high-resolution electron energy analyzer is shown to be necessary to correctly deconvolute the various species in the core level spectra, since binding energy shifts can be small during sulfide formation.

II. EXPERIMENTAL

The present study was performed at beam line UV-8b at the National Synchrotron Light Source at Brookhaven National Laboratory. The sample preparation procedures,[7] electron spectrometer,[8] and monochromator[9] have been described previously. Briefly, clean basal plane [or (0001)] surfaces were produced by cleavage of natural molybdenite crystals in air, followed by annealing at ~975 K for 10 min in the metal deposition chamber (~1×10^{-10} Torr base pressure). This annealing procedure is known to remove virtually all contamination from the surface without formation of defects.[10,11] Photoelectron spectra showed no evidence of either carbon, oxygen, or other impurities on the surface of the samples after the anneal, while LEED showed good quality (0001) - 1 × 1 patterns. The sample preparation chamber was connected to the spectrometer chamber (~3×10^{-11} Torr base pressure), so that the samples could be kept in ultrahigh vacuum (UHV) during transfer between metal deposition and analysis steps.

The instrument resolution is demonstrated by the complete separation of the j = 1/2 and j = 3/2 components of the S-2p doublet for the cleaved MoS_2(0001) surface in Fig. 1e. The instrumental resolution was estimated to be 0.3 eV at 150-225 eV photon energy, and 0.4 eV at 290-300 eV photon energy. The S-2p and Mo-3d core levels were collected for $h\nu$ = 230 and 300 eV, respectively, corresponding to a ~70 eV electron kinetic energy. This ensured that the same electron escape depth (~4Å)[12] was obtained for sampling both the S and the Mo. The Mn-3p and Mo-4p core level spectra were recorded for a photon energy of 290 eV (kinetic energies of ~240 and ~255 eV) while the valence band spectra were collected for photon energies of 152 and 224.7 eV (resulting in escape depths of ~5.5 and ~6.5 Å, respectively). The spectra were normalized by dividing the photoelectron current by the photon intensity determined by measuring the total current resulting from the electron emission from the (carbon contaminated) Au-coated final focusing mirror with an electrometer.

Core level spectra were deconvoluted with Voigt functions using a peak fitting procedure.[7] The Mo-3d doublet was fit by constraining the peak separation and the branching ratio for the 5/2 and 3/2 spin-orbit components to be 3.14 eV and 1.43, respectively, while the corresponding constraints for the S-2p 3/2 and 1/2 spin-orbit components were 1.19 eV and 2.01. These values were derived from spectra for a number of clean MoS_2(0001) surfaces (The branching ratios are different from the theoretical values of 1.50 and 2.00 due to final state effects.)

Manganese (99.995% purity) was evaporated onto the sample surface from a 1/4-in.-diameter tungsten wire basket at a rate of ~12 Å/min. The pressure during deposition was typically in the mid 10^{-10} Torr range. The sample remained at ambient temperature during deposition. Mn film thicknesses were determined by measuring the deposition rate with a quartz crystal microbalance, which could be moved into the position where the sample is located during film growth. This procedure is accurate to within ~50%. After the deposition, and also after subsequent annealing, there was no evidence of carbon or oxygen detected by photoelectron spectroscopy.

The deposition of Mn and subsequent annealing was performed on two separate samples. The spectra displayed herein are from one sample, but are also representative of those for the other sample.

III. RESULTS AND DISCUSSION

A. CORE LEVEL SPECTRA

Figure 2 shows the evolution of the Mn-3p and Mo-4p core levels deposition of Mn on $MoS_2(0001)$ and subsequent annealing. As the Mn is deposited, the Mn peak increases relative to the Mo peak. The Mn film has covered the MoS_2 substrate after deposition of 58 Å Mn (the Mo-4p is present in Fig. 2c, but is difficult to see because of the high relative intensity of the Mn-3p peak). The binding energy and the increased intensity on the high binding energy side of the Mn-3p peak for all coverages indicates that the Mn is primarily in the form of metallic Mn coexisting with a small amount of Mn in a higher oxidation state, possibly as a sulfide. Annealing the 58 Å film to progressively higher and higher temperatures results in reappearance of the Mo-4p peak caused by agglomeration of the Mn layer into islands, which uncovers the substrate. In addition the Mn-3p spectrum shifts ~1.8 eV to higher binding energy with the first anneal, and exhibits a decrease in overall peak width. This shift is consistent with the formation of MnS, since the difference in the Mn-3p binding energies of Mn and MnS has been determined to be in the range of 1.6 eV[13,14] to 2.4 eV.[15] Therefore, the increase in temperature increased the rate of reaction, driving the reaction to equilibrium, which in this case corresponds to sulfide formation, consistent with the negative ΔG_{rxn} mentioned above. After the anneals, the Mo-4p spectrum appears to have shifted to lower binding energy, indicating reduction of the Mo in the MoS_2.

The various species in the Mo-3d and S-2p spectra were deconvoluted by curve fitting, and the results are shown in Fig. 1 for the clean surfaces and three of the depositions (22, 35, and 58 Å; the corresponding spectra for 10 and 50 Å are not shown for reasons of brevity, but their trends are similar to the spectra shown). Initial deposition of Mn caused the Mo-3d peak representing the Mo in the MoS_2 substrate [Mo in the +4 oxidation state, denoted "Mo(substrate)"] to shift -0.3 eV to lower binding energy

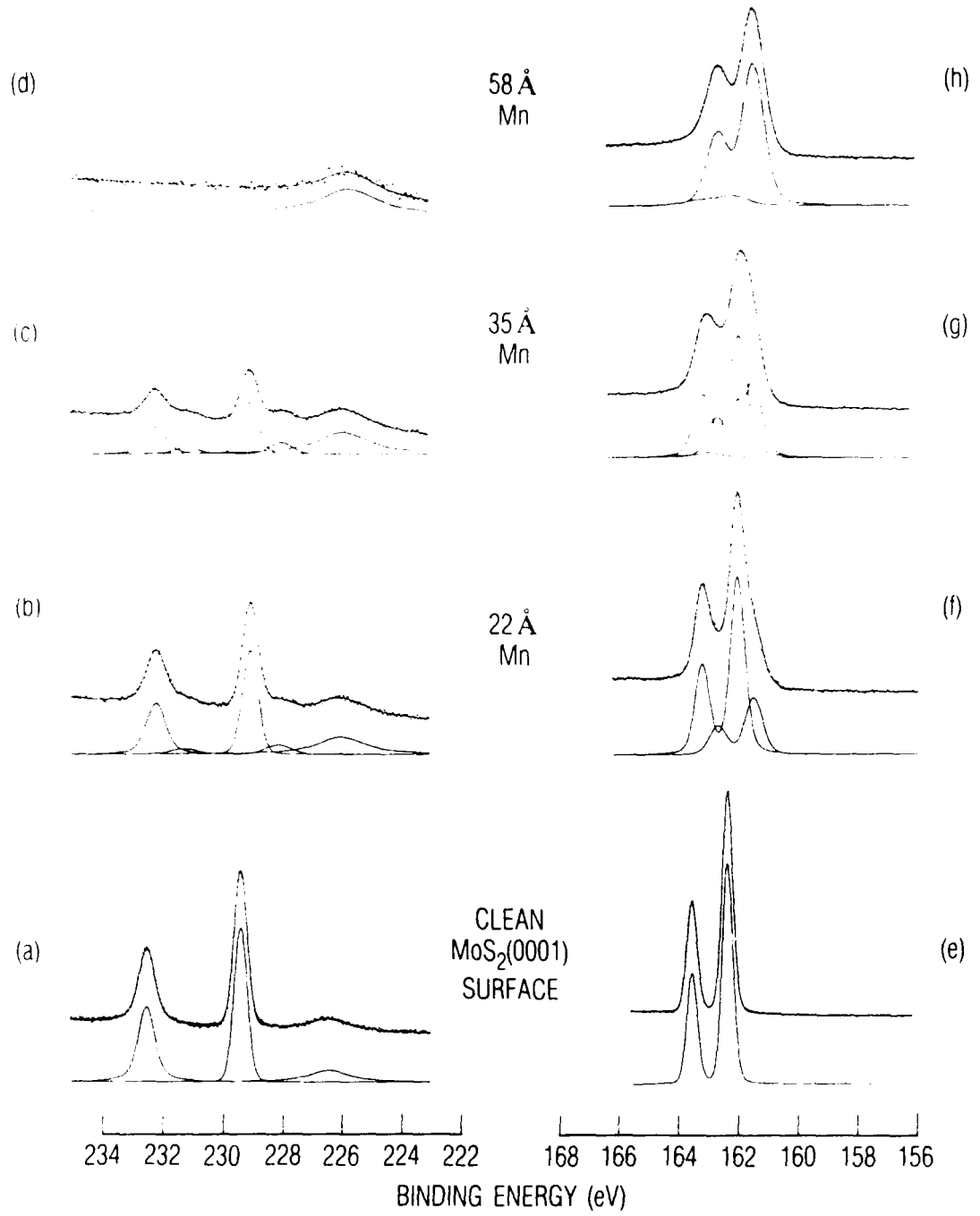

Fig. 1. Mo-3d (a-d) and S-2p (e-h) Core Level Spectra for Deposition of Mn on the $MoS_2(0001)$ Surface. Spectra for the Mo-3d and S-2p core levels were taken with a photon energy of 300 and 230 eV, respectively, resulting in a photoelectron kinetic energy of ~70 eV for both Mo and S photoelectrons. Spectra are shown for (a,e) the clean $MoS_2(0001)$ - 1 surface, and after deposition of (b,f) 22 Å Mn, (c,g) 35 Å Mn, and (d,h) 58 Å Mn. The S-2p peak is at ~226 eV in spectra a-d. Binding energies are relative to Fermi energy E_F.

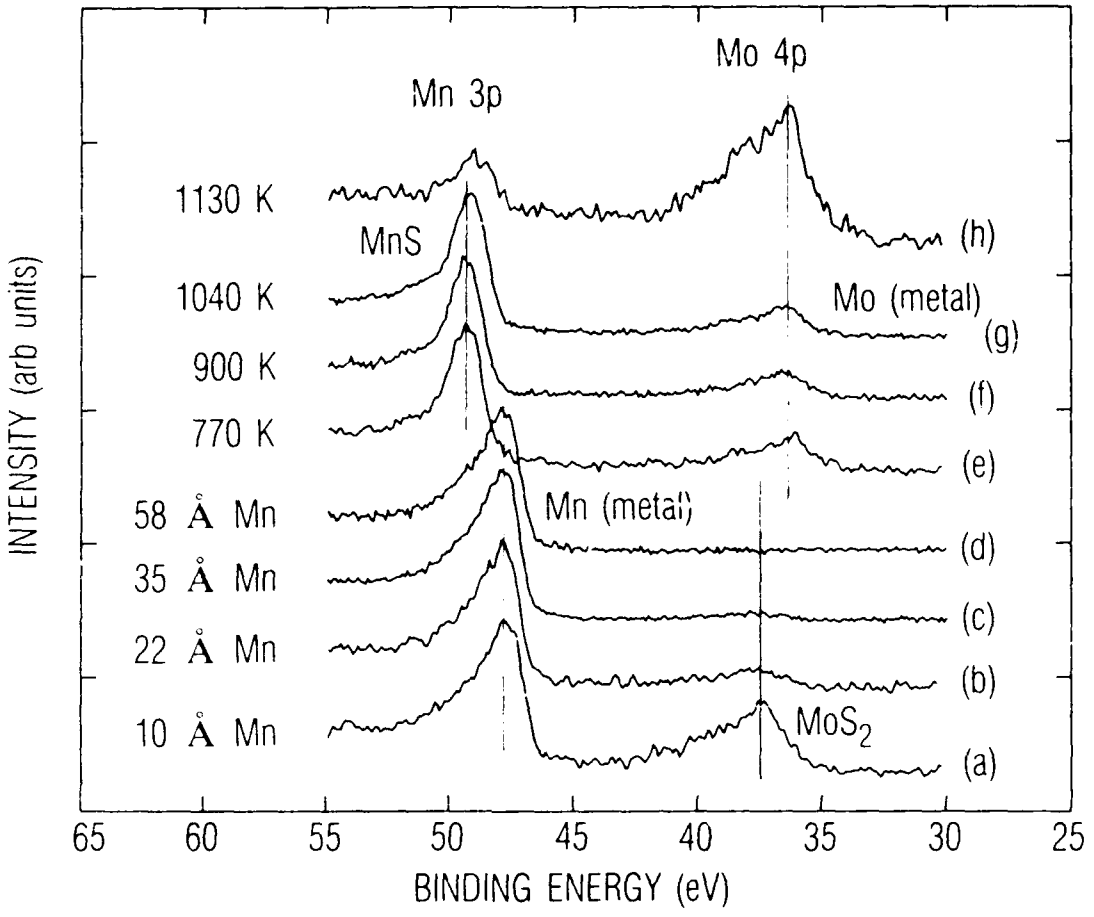

Fig. 2. Mn-3p and Mo-4p Core Level Spectra for Deposition and Annealing of Mn on the MoS_2(0001) Surface. Spectra were taken with a photon energy of 290 eV, resulting in kinetic energies of ~240 and ~255 eV for Mn and Mo photoelectrons, respectively. Spectra are shown for depositions of (a) 10 Å Mn, (b) 22 Å Mn, (c) 35 Å Mn, and (d) 58 Å Mn. Spectra for the 58 Å Mn film are shown after annealing to (e) 770 K, (f) 900 K, (g) 1040 K, and (h) 1130 K. Binding energies are relative to E_F.

due to band-bending (see Fig. 1b and Table I). Also, a reduced Mo species appears whose separation from the Mo(substrate) peak (~1.0 eV, see Table I) corresponds with the formation of metallic Mo [denoted Mo(metal)].[13] The S-2p spectrum deconvolutes clearly into two species (see Fig. 1f): the substrate S [denoted S(substrate) in Table I, and a lower-binding energy species show binding energy (BE) is consistent with that for MnS[15,16] [denoted S(MnS)]. The Mo(metal) peak and the S(MnS) peaks increase in area (relative to the substrate peaks, see Table II) with deposition up to 35 Å thickness (see Fig 1, spectra c and g). For the 58 Å deposition, Mo is not detectable above the noise level in the Mo-3d region (see Fig. 1d), and the S-2p peak exhibits mostly a broadened peak representing the MnS, with a small amount of intensity on the high binding energy side, possibly representing a small amount of S from the MoS_2 substrate (see Fig. 1h).

Table I. Binding Energies of Mo-3d and S-2p Core Levels on the MoS_2(0001) Surface After Mn Deposition[a]

	Mo-3d		S-2p	
	BE	BE	BE	BE
	Mo(substrate)	Mo(metal)	S(substrate)	S(MnS)
Clean surface	229.4 eV	---	162.3	---
Average for 10, 22, and 35 Å Mn	229.07 ±.03	228.04 ±.08	161.93 ±.06	161.40
770 K anneal	228.45 ±.10	227.68	---	161.64
Average for 850, 900, 970 and 1040 K anneals	---	227.90 ±.05	---	161.55 ±.06
1130 K anneal	229.18	227.82	161.94 ±.05	161.25 ±.10

[a]Uncertainty in binding energies is ~0.02 eV, unless otherwise stated.

Table II. Relative Areas of the Mo-3d and S-2p Peaks of the MoS_2(0001) Surface After Mn Deposition

	Mo(metal)/Mo(total)	S(MnS)/S(total)	S(low)[a]/S(total)	S(substrate)/S(total)	S(total)[b]/Mo(total)
Clean surface	0%	0%	---	100%	1.00
Mn coverage					
10 Å	5%	12%	---	88%	1.01
22 Å	12%	15%	---	85%	2.54
35 Å	22%	38%	---	62%	2.99
58 Å	---[c]	91%	---	9%	---[c]
Anneal temp of 58 Å Mn film					
770 K	89%	75%	16%	9%	1.65
900 K	96%	93%	4%	~3%	2.10
1040 K	~100%	85%	11%	~0%	1.50
1130 K	67%	38%	6%	56%	0.74

[a]This ratio represents the "low binding energy" component of the S-2p spectrum, visible only in the annealed samples. The uncertainty in this ratio is ~0.2 times the stated value.

[b]This ratio is expressed relative to the ratio for the clean surface, which is set arbitrarily to a value of 1.00. The uncertainty in the ratios is estimated to be 0.05.

[c]This ratio is undefined because no Mo-3d spectrum was detected for this coverage.

The core level results indicate that the Mn grows on MoS_2(0001) in the Volmer-Weber growth mode[17] [three-dimensional (3D) island formation]. This is indicated by the need to deposit $\tilde{>}$ 50 Å Mn to cause the Mo-3d signal to disappear, much greater than the ~4 Å escape depth for ~70 eV electrons (see Section II). In addition, the Stranski-Krastanov growth mode[18] (growth of one or a few 2D layers followed by 3D island formation) can be ruled out, as the initial deposition of 10 Å Mn resulted in a drop of the Mo(substrate) and S(substrate) peak areas by less than 15% relative to the clean surface. The LEED pattern of the sample does not indicate the

presence of an ordered overlayer film, since deposition of 10, 22, and 35 Å Mn causes an increase in background intensity of the (0001) - 1 × 1 pattern, while for dispositions of 50 and 58 Å Mn, and anneals of 770-1040 K, no pattern is seen at all.

After annealing the 58 Å film to 770 K, the Mo-3d spectrum reappears (see Fig. 3b). This deconvolutes into two doublets. The larger one corresponds to the binding energy for metallic Mo,[13] although it is ~0.2 eV less than for the subsequent anneals to 850 - 1040 K. The smaller doublet corresponds well to MoS_2 with S vacancy defects, or MoS_{2-x}, where $0 < x < 1$.[7] The S-2p doublet (see Fig. 3f) represents mainly MnS, but exhibits a small amount of intensity on the high binding energy side, possibly corresponding to S in the MoS_{2-x} region of the surface, and a lower binding energy species. This lower binding energy species [denoted S(low) in Table II] might represent another sulfide of Mn. It also might represent S adsorbed on the surface of either the Mo(metal) or the MnS. (The adsorption of S on Mo(0001) has been shown to exhibit a lower S-2p binding energy than S in MoS_2[7,19].) When the sample is annealed to higher temperatures, i.e., to 850 and 900 K, the substrate components in both the Mo-3d and S-2_p spectra decrease (see Table II), and have disappeared after the anneal to 970 and 1040 K (see Table II and Fig. 3, spectra c and g). This indicates that the reaction to form MnS has been driven by the increase in temperature, in agreement with the Mn-3p core level results (see Fig. 2, spectra d through g). The decrease in the area of the S(low) doublet at 850 K and 900 K is concurrent with the rise in the S(total):Mo(total) ratio, while the subsequent rise in S(low) at 970 K and 1040 K is concurrent with the fall of the S(total):Mo(total) ratio. The amount of Mo(total) is virtually equal to the amount of Mo(metal) during annealing. Therefore, a change in the amount of S(low) seems to move in the same direction as a change in the amount of Mo(metal). This is consistent with the conclusion that the S(low) species represents S adsorbed on the Mo(metal).

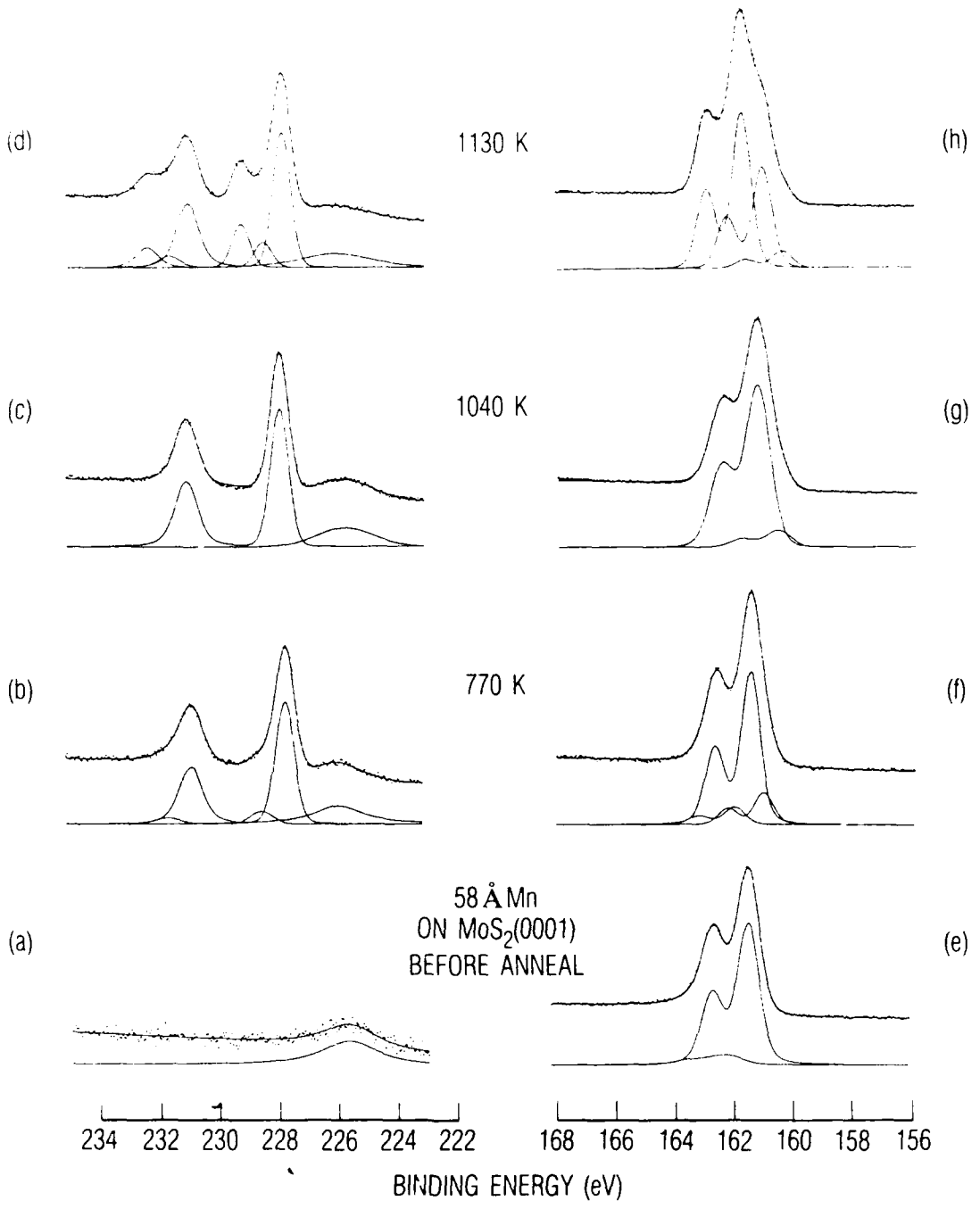

Fig. 3. Mo-3d (a-d) and S-2p (e-h) Core Level Spectra for Annealing of Mn on the MoS_2(0001) Surface. Spectra were taken with same photon energies as in Fig. 1. Spectra are shown for (a,e) the 58 Å Mn film, and after annealing this film to (b,f) 770 K, (c,g) 1040 K, and (d,h) 1130 K. The S-2s peak is at ~226 eV in spectra a-d. Binding energies are relative to E_F.

The drop in the Mo(metal) peak area as the annealing temperature is increased from 770 K to 900 K is due to continued MnS formation (see Section III-B, below), which competes with the Mo(metal) for coverage of the surface. The loss of some of the adsorbed S at this point may also be related to the formation of MnS. The increase in the Mo(metal) peak area between 900 K and 1040 K may be due to partial decomposition of the MnS, which serves as a source for the return of the adsorbed S. S adsorbed on Mo is relatively refractory[19] and, therefore, would not be desorbed at this temperature.

B. VALENCE BAND SPECTRA

Valence band photoelectron spectra were taken for photon energies of 152 eV and 225 eV during depositon of Mn on MoS_2(0001) and subsequent annealing of the samples. Only the 152 eV spectra are reproduced here (see Fig. 4), since the results of the two sets show good agreement. Initial deposition causes shifting of the spectrum ~0.3 eV to lower binding energy (see Fig. 4b), in agreement with the band-bending seen in the core levels. Also, increased intensity from 1 eV to the Fermi level indicates that the surface is becoming metallic due to the presence of metallic Mn. The MoS_2 peak structure is still seen in the 10 Å spectrum, showing that the substrate has not reacted appreciably or been covered by the overlayer. Also, when the metallic edge of the 10 Å spectrum is scaled to coincide with the corresponding metallic edge of the 35 Å spectrum, and the 35 Å spectrum is subtracted from the 10 Å spectrum, the resultant difference spectrum is virtually identical to that for the clean surface, indicating that the reacted layer (i.e., Mn+MnS+Mo) coexists with relatively undisturbed substrate. Therefore, probably no Mn_xMoS_2 compound is formed during deposition. Spectra c and d in Fig. 4 (especially d) correspond well with the valence band spectrum for Mn metal.[15] The 35 Å spectrum (Fig. 4c) exhibits a bit more intensity in the areas of ~4 eV and ~6 eV than the 58 Å spectrum (Fig. 4d). This is due to the persistence of the signal from the substrate (compare Fig. 2, spectra c and d).

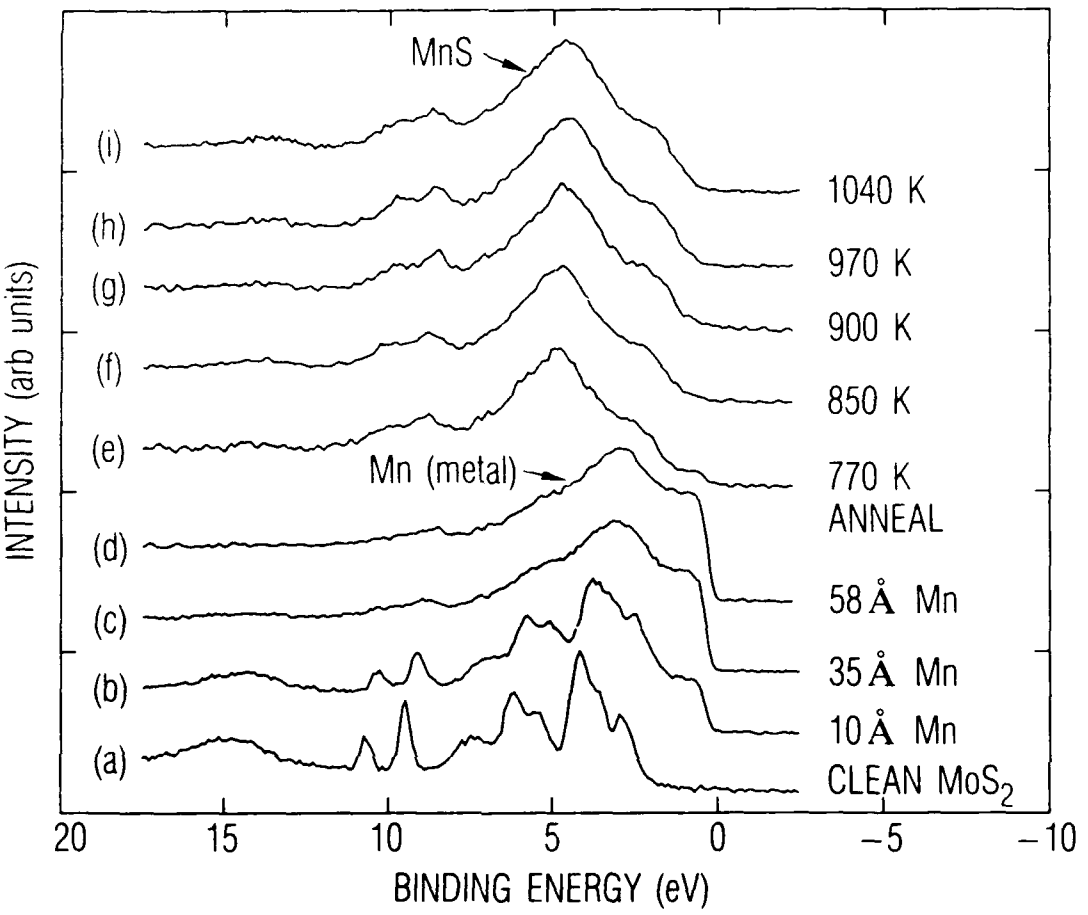

Fig. 4. Valence Band Spectra (h = 152 eV) for Deposition and Annealing of Mn on the MoS_2(0001) Surface. Spectra are shown for (a) the clean MoS_2(0001) - $\bar{1}$ × 1 surface, and after deposition of (b) 10 Å Mn, (c) 35 Å Mn, and (d) 58 Å Mn. Spectra for the 58 Å Mn film are shown after annealing to (e) 770 K, (f) 850 K, (g) 900 K, (h) 970 K, and (i) 1040 K. The two peaks visible at ~9-11 eV result from the S-2p core level doublet produced by second-order light from the monochromator. Binding energies are relative to E_F.

With the anneal to 770 K (see Fig. 4e), a large increase in intensity appears at ~5 eV, due to the formation of MnS (see below) and the reappearance of the substrate. Also, the Mn metal areas of the valence band (at ~1 and ~3 eV) persist, indicating that there is a small amount of unreacted Mn at this annealing temperature. After annealing to 850 K, however, there is no evidence for the existence of unreacted Mn (see Fig. 4f). The spectra for anneals between 850 and 1040 K indicate a mixture of MnS (represented mainly by the peak at ~.5 eV[15,16]) and metallic Mo (peak at ~2 eV[20]), in agreement with the core level spectra (see Fig. 2, spectra f and g; also Fig. 3, spectra c and g). The MnS peak shifts ~0.5 eV to lower binding energy as the temperature is increased from 900 K to 1040 K. This may be due to a phase transition in MnS from the α phase to the β phase[21] or partial decomposition, as mentioned above.

C. FORMATION OF MoS_2(0001) - 2 × 2

After annealing to 1130 K, the substrate (0001) - 1 × 1 LEED pattern reappeared, and also exhibited half-order spots over much of the sample surface, indicating the formation of a surface structure with (0001) - 2 × 2 periodicity. In addition, the core level spectra exhibit large changes in shape (see Fig. 3, spectra d and h). The Mo-3d and S-2p core levels can be deconvoluted into three doublets each. The Mo-3d spectrum (see Fig. 3d) exhibits the reappearance of the Mo(substrate) doublet resulting from MoS_2, coexisting with a large Mo(metal) doublet. In addition, a smaller doublet appears with a binding energy intermediate between these two doublets, which probably represents the 2 × 2 regions of the surface. The S-2p doublet deconvolutes into a large substrate doublet, followed at lower binding energies by a slightly smaller S(MnS) doublet, and a small, lower binding energy doublet. As mentioned above, this lower binding energy doublet might represent adsorbed S, or it might represent S in the 2 × 2 regions of the surface.

Preliminary studies involving the thermal decomposition of the MoS_2(0001) - 1 × 1 surface[22] correlate well with the present results. Annealing to temperatures in excess of 1375 K caused the formation of a

(0001) - 2 × 2 LEED pattern, similar to annealing the $Mn/MoS_2(0001)$ interface to 1130 K in the present study. In addition, the core-level photoelectron spectra of the annealed $MoS_2(0001)$ surface appear similar to those of the annealed $Mn/MoS_2(0001)$ interface.

In a recent study of the $Fe/MoS_2(0001)$ interface,[1] a (0001) - 2 × 2 LEED pattern was observed when the sample was annealed to 1200 K. This result, the results of the present study, and the preliminary thermal decomposition results for the clean surface, indicate that the (0001) - 2 × 2 LEED pattern seen for higher temperature-annealed metal/MoS_2 interfaces is not due to the formation of a $(metal)_xMoS_2$ compound, but rather is due to sulfur vacancy defects in the surface region, produced when the metals react with the MoS_2 to form metal-sulfur compounds. Therefore, these chemically produced defects allow the (0001) - 2 × 2 structure to form at a lower temperature than for the clean surface. In addition, the difference in reactivity between Fe and Mn affects the formation of this structure. Although Fe exhibits some evidence of reactivity with respect to $MoS_2(0001)$,[1,4] the reactivity is considerably less than for Mn on $MoS_2(0001)$.[2] Since there is less deficiency of S in the substrate surface for Fe/MoS_2, a higher temperature (1200 K) is required to produce the (0001) - 2 × 2 defect structure than for Mn (1130 K0.

Although valence band spectra for the 1130 K anneal were not taken with a 152 eV photon energy as in Fig. 4, a spectrum with a 225 eV photon energy (not shown) was taken that exhibits a broad peak with maximum intensity at ~4.5 eV, and higher intensity at ~2 eV than in the previous spectra. The general shape of the spectrum indicates that Mo(metal) and MnS continue to cover some of the surface, with a broad structureless valence band shape indicating disorder in the uncovered areas of the surface that contributed to the (0001) - 1 × 1 and - 2 × 2 LEED patterns.

IV. SUMMARY AND CONSLUSIONS

A core level and valence band photoelectron spectroscopy study was conducted of the Mn/MoS_2(0001) interface. In general, it was shown that Mn reacted with the MoS_2(0001) surface as represented in the overall reaction:

$$Mn + \frac{1}{2} MoS_2 \rightarrow MnS + \frac{1}{2} Mo \qquad (2)$$

Specifically, Mn forms three-dimensional islands on MoS_2, covering the substrate with a complete layer only for an amount of Mn that would have given a thickness equivalent to ~50 Å for layer-by-layer deposition. Reaction (2) initiated for thicknesses $\lesssim$ 10 Å Mn, and was driven by increasing amounts of Mn. The binding energies of the deposition-produced species in the Mn-3p and S-2p core level spectra corresponded to MnS, while the Mo-3d spectra indicated the formation of metallic Mo. Valence band spectra showed that for initial deposition, the partially reacted layer (i.e., Mn+MnS+Mo) formed an abrupt interface with the unreacted substrate.

The reaction was driven by annealing ~50 to ~58 Å Mn films on MoS_2(0001) to temperatures in the range 770 - 1040 K. Analysis of the core levels after annealing to 770 K indicated that the MoS_2 substrate surface was sulfur-deficient, while valence band spectra showed that some unreacted Mn coexisted with a mostly MnS overlayer. The reaction was driven to completion by annealing to temperatures $\gtrsim$ 850 K.

Annealing to temperatures $\gtrsim$ 1130 K resulted in the formation of a MoS_2(0001) - 2 × 2 LEED pattern. The observation of this surface structure is interpreted in terms of a sulfur-vacancy-produced defect structure, rather than a metal-Mo-S compound.

REFERENCES

1. M. Kamaratos, and C. A. Papageorgopoulos, Surf. Sci. 160, 451 (1985).

2. J. R. Lince, D. J. Carre, and P. D. Fleischauer, Phys. Rev. B. 36, 1647 (1987).

3. I. T. McGovern, E. Dietz, H. H. Rotermund, A. M. Bradshaw, W. Braun, W. Radlik, and J. F. McGilp, Surf. Sci. 152/153, 1203 (1985).

4. J. R. Lince, T. B. Stewart, M. M. Hills, P. D. Fleischauer, J. A. Yarmoff, and A. Taleb-Ibrahimi, Surf. Sci. (submitted).

5. M. Kamaratos, and C. A. Papageorgopoulos, Appl. Surf. Sci, 29, 279 (1987).

6. C. A. Papageorgopoulos and M. Kamaratos, Surf. Sci. 164, 353 (1985).

7. J. R. Lince, T. B. Stewart, M. M. Hills, P. D. Fleischauer, J. A. Yarmoff, and A. Taleb-Ibrahimi, Surf. Sci. 210, 387 (1989).

8. D. E. Eastman, J. J. Donelon, N. C. Hein, and F. J. Himpsel, Nucl. Inst. Meth. 172, 327 (1980).

9. F. J. Himpsel, Y. Jugnet, D. E. Eastman, J. J. Donelon, D. Grimm, G. Landgren, A. Marx, J. F. Morar, C. Oden, and R. A. Pollak, Nucl. Instrum. Meth. 222, 107 (1984).

10. J. C. McMenamin and W. E. Spicer, Phys. Rev. B 16, 5474 (1977).

11. J. Bandet, A. Malvand, and Y. Quemener, J. Phys. C 13, 5657 (1980).

12. Calculated from formula in S. Tanuma, C. J. Powell, and D. R. Penn, Surf. Sci 192, L849 (1987), which was for electron kinetic energies of 200 eV and higher.

13. C. D. Wagner, W. M. Riggs, L. E. Davis J. F. Moulder, and G. E. Muilenberg, eds., X-ray Photoelectron Spectroscopy (Perkin-Elmer, Eden Prairie, 1979).

14. H. F. Franzen, M. X. Umaña, J. R. McCreary, and R. J. Thorn, J. Solid State Chem. 18, 363 (1976).

15. H. F. Franzen, and C. Sterner, J. Solid State Chem. 25, 227 (1978).

16. H. van der Heide and C. F. van Bruggen, Mater. Res. Bull. 17, 1517 (1982).

17. M. Volmer and A. Weber, Z. Phys. Chem. 119, 277 (1926).

18. I. N. Stranski and L. Krastanov, Acad. Wiss. Math.-Nat. K1 IIb 146, 797 (1938).

19. A. Gellman, W. T. Tysoe, F. Zaera, and G. A. Somorjai, Surf. Sci. 191 271 (1987).

20. S. J. Atkinson, C. R. Brundle, and M. W. Roberts, Chem. Phys. Lett. 24, 175 (1974).

21. M. Hansen, Constitution of Binary Alloys (McGraw-Hill, New York, 1958), p. 950.

22. J. R. Lince (unpublished results).

LABORATORY OPERATIONS

The Aerospace Corporation functions as an "architect-engineer" for national security projects, specializing in advanced military space systems. Providing research support, the corporation's Laboratory Operations conducts experimental and theoretical investigations that focus on the application of scientific and technical advances to such systems. Vital to the success of these investigations is the technical staff's wide-ranging expertise and its ability to stay current with new developments. This expertise is enhanced by a research program aimed at dealing with the many problems associated with rapidly evolving space systems. Contributing their capabilities to the research effort are these individual laboratories:

Aerophysics Laboratory: Launch vehicle and reentry fluid mechanics, heat transfer and flight dynamics; chemical and electric propulsion, propellant chemistry, chemical dynamics, environmental chemistry, trace detection; spacecraft structural mechanics, contamination, thermal and structural control; high temperature thermomechanics, gas kinetics and radiation; cw and pulsed chemical and excimer laser development including chemical kinetics, spectroscopy, optical resonators, beam control, atmospheric propagation, laser effects and countermeasures.

Chemistry and Physics Laboratory: Atmospheric chemical reactions, atmospheric optics, light scattering, state-specific chemical reactions and radiative signatures of missile plumes, sensor out-of-field-of-view rejection, applied laser spectroscopy, laser chemistry, laser optoelectronics, solar cell physics, battery electrochemistry, space vacuum and radiation effects on materials, lubrication and surface phenomena, thermionic emission, photosensitive materials and detectors, atomic frequency standards, and environmental chemistry.

Computer Science Laboratory: Program verification, program translation, performance-sensitive system design, distributed architectures for spaceborne computers, fault-tolerant computer systems, artificial intelligence, microelectronics applications, communication protocols, and computer security.

Electronics Research Laboratory: Microelectronics, solid-state device physics, compound semiconductors, radiation hardening; electro-optics, quantum electronics, solid-state lasers, optical propagation and communications; microwave semiconductor devices, microwave/millimeter wave measurements, diagnostics and radiometry, microwave/millimeter wave thermionic devices; atomic time and frequency standards; antennas, rf systems, electromagnetic propagation phenomena, space communication systems.

Materials Sciences Laboratory: Development of new materials: metals, alloys, ceramics, polymers and their composites, and new forms of carbon; nondestructive evaluation, component failure analysis and reliability; fracture mechanics and stress corrosion; analysis and evaluation of materials at cryogenic and elevated temperatures as well as in space and enemy-induced environments.

Space Sciences Laboratory: Magnetospheric, auroral and cosmic ray physics, wave-particle interactions, magnetospheric plasma waves; atmospheric and ionospheric physics, density and composition of the upper atmosphere, remote sensing using atmospheric radiation; solar physics, infrared astronomy, infrared signature analysis; effects of solar activity, magnetic storms and nuclear explosions on the earth's atmosphere, ionosphere and magnetosphere; effects of electromagnetic and particulate radiations on space systems; space instrumentation.